

A Diffusion Model for Coefficient Identification during Growth of Nitrides

J. Bernal, A. Medina, L. Béjar, S. Rangel, A. Juanico

Abstract—Nitrogen diffusion coefficients during the growth of nitrided concomitant layers produced by microwave post-discharge nitriding were estimated through an inverse problem model. Diffusion coefficients in each phase are estimated by setting the inverse problem associated with growth of compact nitrided layer γ' -Fe₄N₁, austenite layer γ , and a nitrogen diffusion zone in ferrite. The evolution of nitrogen concentration profile from supersaturated ferrite to the formation of compact nitride layers is described. Nitrogen concentrations in each phase and diffusion zone are not considered to be bounded by their solubility limits. Evolution for large periods (quasi-steady periods), coincides with layer growth evolution considered in mass balance models.

Keywords— Coefficient, Diffusion, Nitriding Quasy-Steady.

I. INTRODUCTION

Nitriding is a thermo-chemical treatment for the introduction of nitrogen to the surface of metal parts. Generally this surface treatment has been accomplished with no reduction in the core properties of the part. This technology has been employed to increase superficial hardness, as well improve fatigue strength and to improve resistance to wear and corrosion. This method was used for the first time in late 1920 and since then has steadily increased its application because it can be applied to a wider range of steels other than originally thought. The thermochemical nitriding treatments produce an important improvement in the mechanical, tribological and chemical properties in steel, thus enhancing their fatigue corrosion and wear resistance, the wearing down and the corrosion [1-4]. Nitriding processes involve several sensitive issues as the evolution of the concentration of nitrogen in the surface and the evolution of the concentration of nitrogen within the metal [5-8].

The evolution of the nitrogen concentration in the surface is inherent to the process. In the processes where the diffusion takes place through a thermochemical balance between a gaseous mixture and the solid, for example mixtures with ammonia, the nitrogen concentration in the surface depends on the nitrogen potential [9-11].

Among the nitriding process can distinguish the gas nitriding, plasma nitriding or pulsed discharge [14-20], in the processes attended by weakly ionized plasma, the surface is the residence of the pulverization events, adsorption and diffusion [19-21]. The nitrogen concentration in the surface evolves quickly. The nitrogen concentration in the surface corresponds to a dynamic balance between pulverization

towards the atmosphere and the diffusion towards the solid.

It is important to know the phases present, their morphology and developed layer thickness on the substrate, which are controlled by the variables involved in the process. The formation of compacted layers depends on the reactions that take place between the atmosphere and the substrate, in particular the production of species. Absorbed species density determines the concentration of nitrogen in the surface and the formation of "early stage" (initial states) that precedes the development of compact layers on iron substrates. It is therefore an interest for us to understand the formation of these phases, through the analysis of products obtained in experiments that subsequently lead to a proposed mechanism of formation of phases.

An immediate purpose of the study of the phenomena of nitriding is the automation and control of it. To this end mathematical models are needed of the phenomenon and it is also necessary to have the solution, exact or approximate these models. In the mathematical simulation of the diffusion of nitrogen in the iron or the steel reported in literature, the nitrogen concentration in the surface is assumed constant from the beginning of the treatment [22,23], consequently is considered that the thickness of the layers is zero for the initial moment.

The control or automation of the nitriding processes depends on the instrumentation necessary to identify the concentration of nitrogen in the surface as well as of a mathematical model adapted to estimate the growth kinetics of compact concomitant nitride layers. On the other hand, the understanding and interpretation of the mechanisms of transport of mass in the solid require of the experimental validation of the diffusion coefficients.

The calculation of the coefficients of diffusion with base in experimental results has assumed a profile of parabolic growth for each layer from the beginning of the process, nevertheless the nitrogen concentration take different way in each process and depends of each one. If the nitrogen concentration in the surface evolves slowly, the condition of parabolic regime will not be observed during the initial stages, in addition will limit the precision of the calculation of the diffusion coefficients.

The nitriding attended by post-discharge, generates an atmosphere with excited neutral species or dissociated, these species produce a fast evolution of the nitrogen concentration in the surface [24-27].

It has been observed that the atomic nitrogen presence in the post-discharge significantly increases the transference of mass to the solid in comparison with other processes. With base in obtained experimental results in iron nitriding under

atmosphere produced by post-discharge microwaves, the present work considers a one-dimensional model of kinetics of layer growth, studies the inverse problem to estimate the diffusion coefficients of each phase from the consideration of the stabilization of the layers after a certain period of treatment, such consideration is also justified experimentally and taking into account the analytical expression from the kinetics of layer growth.

The experimental results generated by means of treatments attended by post-discharges generated by a microwave source also allow, to accurately determining values for the diffusion coefficients on the basis of the one-dimensional model of growth kinetics of concomitant nitride layers.

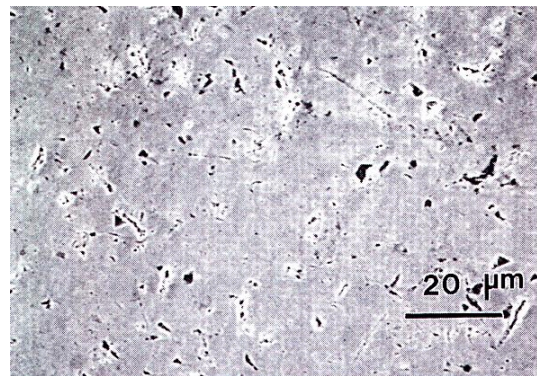
II. EXPERIMENTAL PROCEDURE

Samples were obtained from a commercial ARMCO iron bar (25.4mm in diameter and 7mm thick. Mn 880ppm; C and P, 200ppm; and S 150ppm). Nitriding was carried out in post discharge microwave-generated plasma described elsewhere [25]. The general sequence of the nitriding experiments started with heating of the sample to 770 K in a tubular resistance furnace in a non oxidized and non nitriding atmosphere composed of 26Ar-80H₂ sccm at a total pressure of 900 Pa.

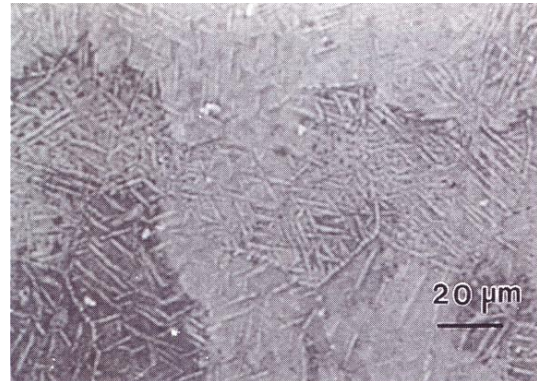
The applied and reflected power was 200W and 65 respectively and the distance from the discharge point was 7cm. Upon reaching the prescribed temperature, the atmosphere was switched to a mixture of 300N₂-26Ar-80H₂ at 1200 Pa and recording of the nitriding time started. After the nitriding time was completed, the atmosphere was switched back to the initial non-oxidizing, non-nitriding atmosphere.

III. CHARACTERIZATION

An overview of the morphology of the phase γ' -Fe₄N_{1-x} by optical microscopy (OM) is shown in Figs. 1 (a-d). The micrographs correspond to samples treated for (a) 30, (b) 60 (c) 180; y (d) 600 s. They allow us to observe more closely the evolution of the microstructure on the surface of the sample based on time and under conditions of constant treatment. Fig. 1 shows the evolution of the surface structure with the nitriding time in a series of SEM top views. After 30 s of nitriding, very small needles are observed on the surface (Fig. 1a). However, 30 s later; Fig. 1b shows that the surface is already fairly covered with nitrides, although some areas within the grains are still free of precipitates. After nitriding for 180 s, the surface view of Fig. 1c depicts an almost continuous network of needles. Finally, Fig. 1d, which corresponds to 600 s of treatment, displays a surface heavily covered with nitrides.



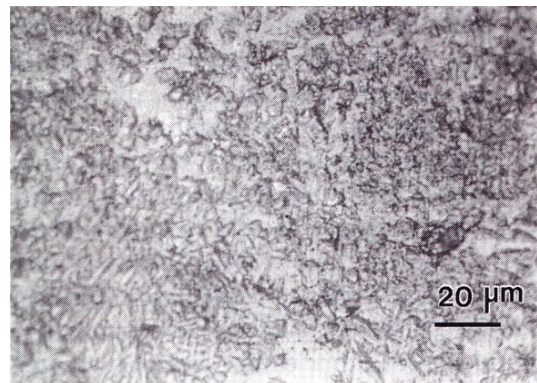
(a)



(b)



(c)



(d)

Fig.1. Evolution of the surface structure nitrided from a top view of the sample: (a) 30; (b) 60, (c) 180; and (d) 600 s.

It should be noted in these micrographs that the size of the needles does not change appreciably with time and that the coverage of the surface by nitrides mainly occurs by continuous needle nucleation, although some contribution also arises from branching of the γ' -Fe₄N_{1-x} precipitates. The details of growth by branching are clearly displayed in Fig. 2, which also shows that the needles have a prismatic shape.



Fig. 2. Details of surface needle growth of γ' -Fe₄N_{1-x} by branching

The evolution of the nitride layer can be followed in Fig. 3(a-d), which is a series of cross-sectional views corresponding to the surface micrographs of Fig. 1.

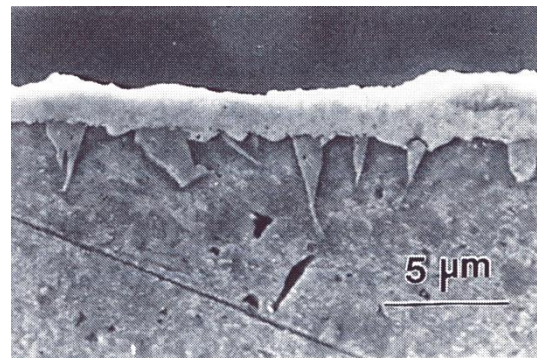
The micrograph of cross section shown in Fig. 3a shows the growth phase γ' -Fe₄N_{1-x}, whose morphology resembles that of a tooth or sharp cone. The thickness at the root of the cones corresponds roughly to the thickness of the needle on the surface, reaching lengths of 2 to 4 μ m and its size depends on the local value of the free energy in the growth zone. Gibbs free energy is the function that represents the energy stability of the phase, this in turn can be represented by the chemical potential. The migration of nitrogen in solid solution and the concentration gradient in the substrate depend on this energy. The crossing of the precipitates in some areas comes from the grain boundaries, regions of higher energy for nucleation and growth of precipitates.

The micrograph in Figure 3.b shows the phase thickening γ' -Fe₄N_{1-x} in a cone shape, however, still can't see any noticeable change in its length. The initial coalescence between the precipitates begins to take shape from the surface, as a consequence of increasing the treatment period. The growth profile of the acute phase γ' -Fe₄N_{1-x}, with respect to its depth, is also an indicator of high initial concentration gradient that forms between the surface and solid.

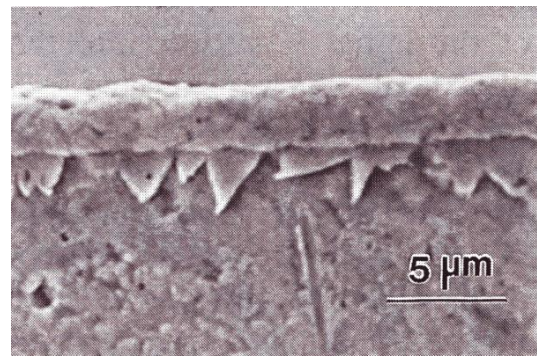
In the micrograph shown in Figure 3.c can be seen as a clear shift in terms of the initial morphology of the cone-shaped nitrides. The sharp profile of the cones has practically disappeared, the thickening resulted in a globular-shaped structure present along the cut and which promotes the coalescence of nitrides, forming the beginning of an irregular front. In this area, the flow of N governed by the chemical equilibrium between phases leads to the evolution of a plane front growth.

Figure 3.d shows a cross-sectional micrograph of the surface nitrided at 600 s. Note the initial formation of a globular precipitates irregular front that tends to form a

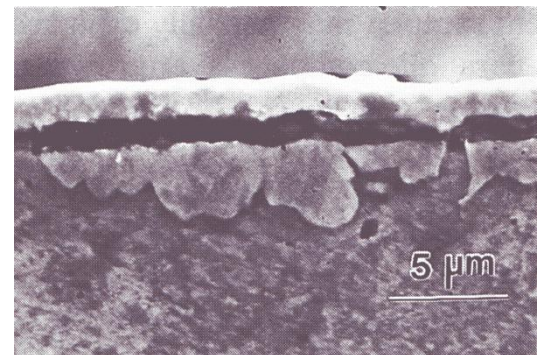
compact layer from the coalescence of these. The average thickness of the front of γ' -Fe₄N_{1-x} is approximately 4 μ m.



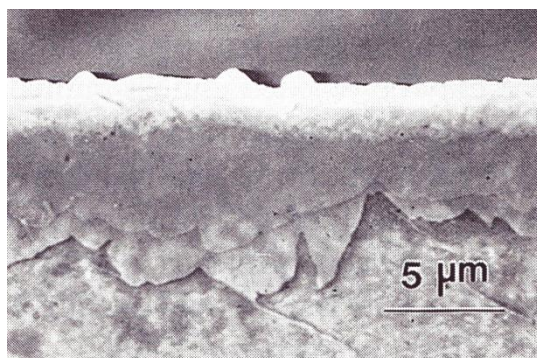
(a)



(b)



(c)



(d)

Fig.3. Cross sectional views corresponding to the surface micrographs: (a) 30; (b) 60; (c) 180; and (d) 600 s.

Fig. 4 shows the diffraction patterns obtained from X-ray analysis of the sample nitrated for a period of 180 s. We can see signs that clearly identify the presence γ' -Fe₄N_{1-x} on the surface. It also shows the presence of meta-stable phase α'' , which precipitated during cooling α . And obviously we can see the peaks corresponding to the ferrite matrix α iron in greater number.

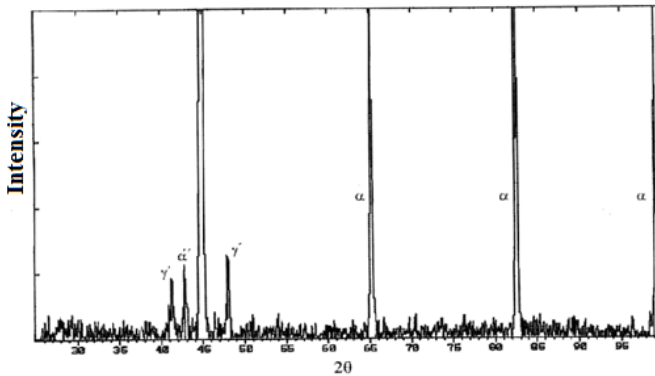


Fig. 4. Pattern of X-ray diffraction of the sample nitrated for 180 s.

Fig. 5 presents a cross-sectional view of a sample nitrated for 120 min under the conditions described previously. The nitrides below the compact nitrides layers precipitated during cooling of the sample due to the desaturation of the ferrite, the width of this zone is between 40 to 50 μ m, and however the diffusion zone of nitrogen in the ferrite is near 3 mm.

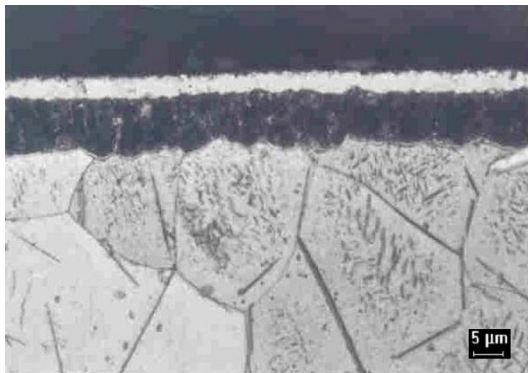


Fig.5. Cross sectional view of a nitride iron sample in postdischarge conditions.

Fig. 6 presents a schematic representation of the evolution of the surface concentration C as a function of time, which is the initial concentration profile of the process. This figure show that a certain time t^* is necessary to precipitate the γ' phase corresponding to limit of the solubility of this phase in the diagram iron-nitrogen.

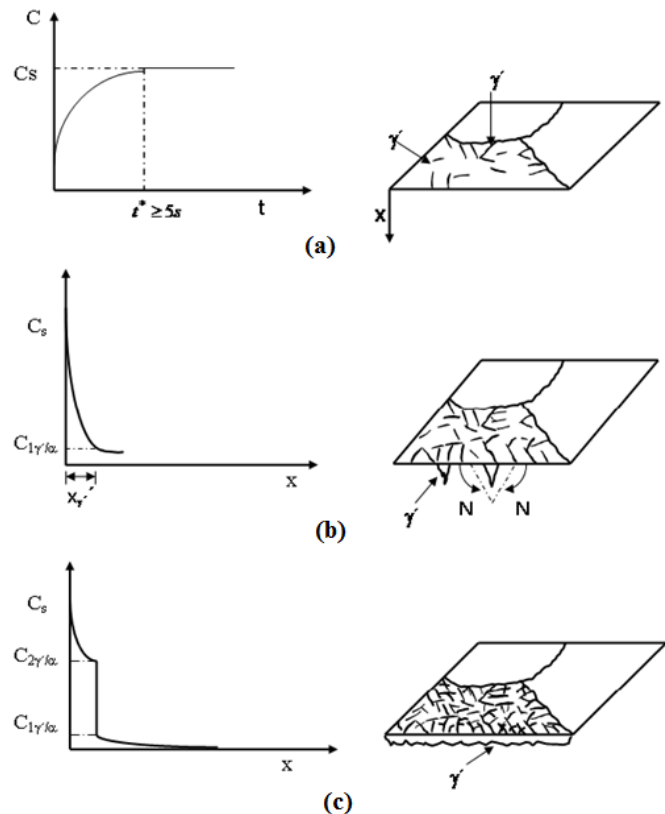


Fig.6. Sequence of initial nitride formation. (a) evolution of the surface concentration. (b) N concentration profile and surface structure right after C_s is reached. (c) Nitrogen concentration profile and initial stage of formation of the flat front by coalescence of nitrides

IV. MODEL AND ITS CONSEQUENCES

Let us propose a mathematical model which describes the layers growth during the post-discharge nitriding process. We suppose that the diffusion is one dimensional and planar and the temperature at every point in the specimen is identical during the whole process. This model presents five steps. The first step corresponds to a normal diffusion process which takes place before the formation of the layers γ' , γ and α .

The first step ends when the surface reaches the concentration C_s at a time t^* (Fig. 6a). This step is modeled by

$$\frac{\partial C}{\partial t} = D \frac{\partial^2 C}{\partial x^2} \quad , \quad 0 < x < +\infty \quad , \quad t > 0 \tag{1}$$

$$C(x,0) = C_0 \quad , \quad 0 < x < +\infty \tag{2}$$

$$\frac{\partial C}{\partial x}(0,t) = \frac{\alpha}{D} [C - C_{eq}]|_{x=0} \quad , \quad t > 0 \tag{3}$$

$$\lim_{x \rightarrow +\infty} C(x,t) = 0 \quad , \quad t > 0 \tag{4}$$

Where α is the constant of the kinetic reaction and $C(x,t)$ represents the concentration of N .

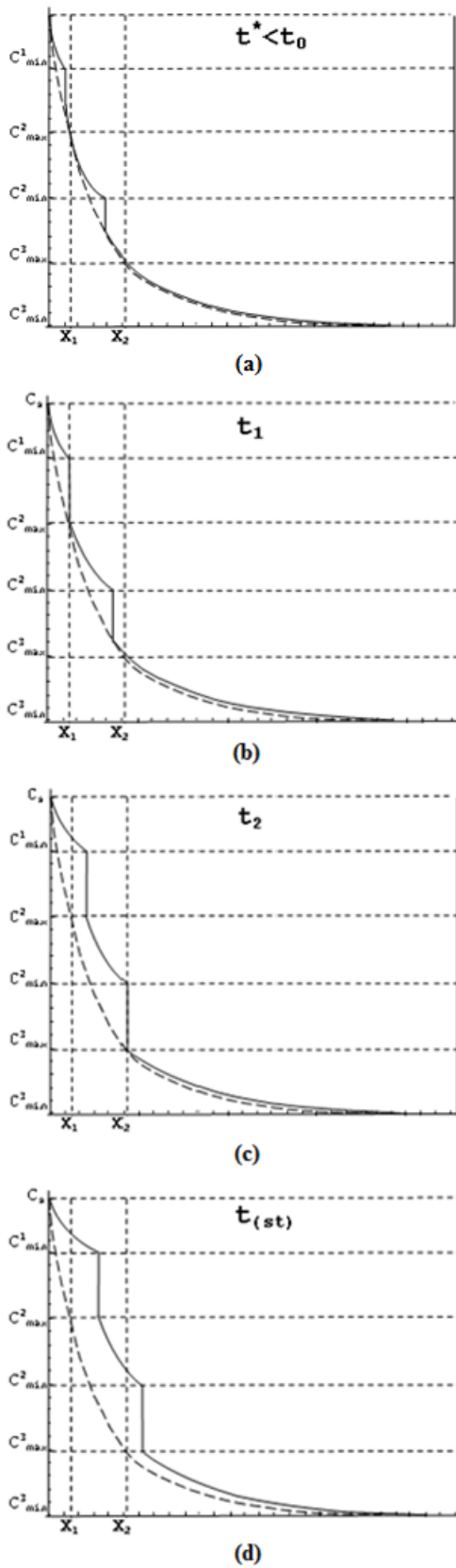


Fig. 7. Schematic representation of concentration gradient as a function of depth for the case of two compact nitride layers where nitrogen is in solution in ferrite.

The solution of (1)-(4) is given by

$$\frac{C - C_{eq}}{C_0 - C_{eq}} = \operatorname{erf}\left(\frac{x}{2(Dt)^{1/2}}\right) + \exp\left(\frac{\alpha}{D}x + \frac{\alpha^2}{D}t\right) \quad (5)$$

$$\operatorname{erfc}\left(\frac{x}{2(Dt)^{1/2}} + \frac{\alpha}{D^{1/2}}t^{1/2}\right)$$

where:

$$\operatorname{erf} x \equiv \frac{2}{\sqrt{\pi}} \int_0^x e^{-\xi^2} d\xi \quad (6)$$

$$\operatorname{erfc} x \equiv 1 - \operatorname{erf} x = \frac{2}{\sqrt{\pi}} \int_x^{+\infty} e^{-\xi^2} d\xi \quad (7)$$

A certain time t^* should pass for the concentration to reach the umbra value C_s , which follows from:

$$\frac{C_s - C_{eq}}{C_0 - C_{eq}} = \exp\left(\frac{\alpha^2}{D}t^*\right) \operatorname{erfc}\left(\frac{\alpha}{D^{1/2}}(t^*)^{1/2}\right) \quad (8)$$

Let us put:

$$f(x) \equiv C(x, t^*) = C_{eq} + (C_0 - C_{eq}) \left\{ \operatorname{erf}\left(\frac{x}{2(Dt)^{1/2}}\right) + \exp\left(\frac{\alpha}{D}x + \frac{\alpha^2}{D}t^*\right) \operatorname{erfc}\left(\frac{x}{2(Dt)^{1/2}} + \frac{\alpha}{D^{1/2}}(t^*)^{1/2}\right) \right\} \quad (9)$$

$f(x)$ denotes the concentration initial profile when the layers formation begins.

The second step contains the beginning of the layers and interface formation (Fig. 7a) and is modeled by:

$$\frac{\partial C_1}{\partial t} = D_1 \frac{\partial^2 C_1}{\partial x^2}, 0 < x < x_{\gamma'}, t^* < t < t_1 \quad (10)$$

$$C_1(x, t^*) = f(x), 0 < x < x_{\gamma'} \quad (11)$$

$$C_1(0, t) = C_s, t > t^* \quad (12)$$

$$\frac{\partial C_1}{\partial x}(x_{\gamma'}, t) = 0, t^* < t < t_1 \quad (13)$$

$$\frac{\partial C_2}{\partial t} = D_2 \frac{\partial^2 C_2}{\partial x^2}, x_{\gamma'} < x < x_{\gamma}, t^* < t < t_1 \quad (14)$$

$$C_2(x, t^*) = f(x), x_{\gamma'} < x < x_{\gamma} \quad (15)$$

$$C_2(x_{\gamma}, t) = C_{max}^2, t > t^* \quad (16)$$

$$\frac{\partial C_2}{\partial x}(x_{\gamma}, t) = 0, t^* < t < t_1 \quad (17)$$

$$\frac{\partial C_3}{\partial t} = D_3 \frac{\partial^2 C_3}{\partial x^2}, x_\gamma < x < x_\alpha, t^* < t < t_1 \quad (18)$$

$$C_3(x, t^*) = f(x) \quad , \quad x_\gamma < x < x_\alpha \quad (19)$$

$$C_3(x_\gamma, t) = C_{\max}^3 \quad , \quad t > t^* \quad (20)$$

$$\frac{\partial C_3}{\partial x}(x_\alpha, t) = 0 \quad , \quad t^* < t < t_1 \quad (21)$$

Where: $x_{\gamma'}$, x_γ , x_α are defined through

$$f(x_{\gamma'}) = C_{\max}^2, f(x_\gamma) = C_{\max}^3, f(x_\alpha) = C_{\min}^3 \quad \text{and}$$

$C_{\max}^i, i = 2, 3$ are the largest values of the concentration C

at the layers γ, α respectively. Mean while t_1 is defined by

$$C_1(x_{\gamma'}, t_1) = C_{\min}^1, \text{ the smallest value of } C \text{ at the layer } \gamma'$$

During the third step layers γ', γ grow and the interface between them moves following a moving boundary problem behavior (Fig. 7b)

$$\frac{\partial C_1}{\partial t} = D_1 \frac{\partial^2 C_1}{\partial x^2}, 0 < x < \xi(t), t_1 < t < t_2 \quad (22)$$

$$\frac{\partial C_2}{\partial t} = D_2 \frac{\partial^2 C_2}{\partial x^2}, \xi_1(t) < x < x_\gamma, t_1 < t < t_2 \quad (23)$$

$$C_1(0, t) = C_s \quad , \quad t > t_1 \quad (24)$$

$$C_1(\xi_{1-0}(t), t) = C_{\min}^1, C_2(\xi_{1+0}(t), t) = C_{\max}^2 \quad (25)$$

$$(C_{\min}^1 - C_{\max}^2) \frac{d\xi_1}{dt} = -D_1 \frac{\partial C_1}{\partial x}(x, t) \Big|_{x=\xi_{1-0}} \quad (26)$$

$$+ D_2 \frac{\partial C_2}{\partial x} \Big|_{x=\xi_{1+0}}$$

$$\frac{\partial C_2}{\partial x}(x_\gamma, t) = 0 \quad , \quad t_1 < t < t_2 \quad (27)$$

Here t_2 is defined by $C_2(x_\gamma, t_2) = C_{\min}^2$, the smallest value of C at the layer γ . The layer α follows an standard diffusion process.

$$\frac{\partial C_3}{\partial t} = D_3 \frac{\partial^2 C_3}{\partial x^2}, x_\gamma < x < x_\alpha, t_1 < t < t_2 \quad (28)$$

$$C_3(x, t_1) = f(x) \quad , \quad x_\gamma < x < x_\alpha \quad (29)$$

$$C_3(x_\gamma, t) = C_{\max}^3 \quad , \quad t > t_1 \quad (30)$$

$$\frac{\partial C_3}{\partial x}(x_\alpha, t) = 0 \quad , \quad t_1 < t < t_2 \quad (31)$$

By the end of this step the three layers are completely formed.

The fourth step corresponds to the growth of the layers and the movement of the interfaces according to the following moving boundary problem (Fig. 7c).

$$\frac{\partial C_1}{\partial t} = D_1 \frac{\partial^2 C_1}{\partial x^2}, 0 < x < \xi_1(t), t_2 < t < t_3 \quad (32)$$

$$\frac{\partial C_2}{\partial t} = D_2 \frac{\partial^2 C_2}{\partial x^2}, \xi_1(t) < x < \xi_2(t), t_2 < t < t_3 \quad (33)$$

$$\frac{\partial C_3}{\partial t} = D_3 \frac{\partial^2 C_3}{\partial x^2}, \xi_2(t) < x < \xi_3(t), t_2 < t < t_3 \quad (34)$$

$$C_1(0, t) = C_s \quad , \quad t > t_2 \quad (35)$$

$$C_i(\xi_{i-0}(t), t) = C_{\min}^i, \quad (36)$$

$$C_{i+1}(\xi_{i+0}(t), t) = C_{\max}^{i+1} \quad , \quad i = 1, 2$$

$$(C_{\min}^i - C_{\max}^{i+1}) \frac{d\xi_i}{dt} = -D_i \frac{\partial C_i}{\partial x}(x, t) \Big|_{x=\xi_{i-0}} \quad (37)$$

$$+ D_{i+1} \frac{\partial C_{i+1}}{\partial x} \Big|_{x=\xi_{i+0}} \quad , \quad i = 1, 2$$

$$C_{\max}^3 \frac{d\xi_i}{dt} = -D_3 \frac{\partial C_3}{\partial x}(x, t) \Big|_{x=\xi_{3-0}} \quad (38)$$

and t_3 is such that $C_3(x_\alpha, t_3) = C_{\min}^3$, the smallest value of C at the layer α . Notice that we are assuming $t_1 < t_2 < t_3$, i.e. the interfaces stabilize in the indicated order.

The fifth and last step corresponds to a period previous to the layers growth “stabilization”, where the layers and interfaces follow the full picture of a moving boundary behavior (Fig. 7d).

$$\frac{\partial C_1}{\partial t} = D_1 \frac{\partial^2 C_1}{\partial x^2}, 0 < x < \xi_1(t), t_3 < t < t_4 \quad (39)$$

$$\frac{\partial C_2}{\partial t} = D_2 \frac{\partial^2 C_2}{\partial x^2}, \xi_1(t) < x < \xi_2(t), t_3 < t < t_4 \quad (40)$$

$$\frac{\partial C_3}{\partial t} = D_3 \frac{\partial^2 C_3}{\partial x^2}, \xi_2(t) < x < \xi_3(t), t_3 < t < t_4 \quad (41)$$

$$C_1(0, t) = C_s \quad , \quad t > t_3 \quad (42)$$

$$C_i(\xi_{i-0}(t), t) = C_{\min}^i, \quad (43)$$

$$C_{i+1}(\xi_{i+0}(t), t) = C_{\max}^{i+1} \quad , \quad i = 1, 2$$

$$(C_{\min}^i - C_{\max}^{i+1}) \frac{d\xi_i}{dt} = -D_i \frac{\partial C_i}{\partial x}(x, t) \Big|_{x=\xi_{i-0}} \quad (44)$$

$$+ D_{i+1} \frac{\partial C_{i+1}}{\partial x} \Big|_{x=\xi_{i+0}} \quad , \quad i = 1, 2$$

$$C_{\max}^3 \frac{d\xi_i}{dt} = -D_3 \frac{\partial C_3}{\partial x}(x, t) \Big|_{x=\xi_{3-0}} \quad (45)$$

Once fifth step is over for large time t_4 , the layers growth become negligible, which is justified from experimental essays and also analytically: interfaces move with velocities proportional to $1/\sqrt{t}$, which become smaller for large values of time. So the process arrives to a quasi-stationary stage, where variation $\frac{\partial C}{\partial t}$ is very small. Moreover, from the fact in every stage diffusion equation fulfills:

$$\frac{\partial C_i}{\partial t} = D_i \frac{\partial^2 C_i}{\partial x^2} \tag{46}$$

and the rate of change of the concentration is positive, then $\frac{\partial^2 C_i}{\partial x^2} \geq 0$ and C_i for every t is a convex function in x , which is also decreasing, reaches its maximum and minimum values at the beginning and at the end of the phase respectively.

V. SIMULATION OF THE CONCENTRATION PROFILE IN THE QUASI-SATATIONARY STAGE

We propose:

$$C_i(x) = a_i(x - x_i)^{m_i} + b_i(x - x_i) + c_i, \quad i = 1, 2, 3 \tag{47}$$

where x_i is the depth of which reaches each phase when quasi-stabilizes (experimental observation). m_i (integers greater or equal than two), $a_i, b_i, c_i, i = 1, 2, 3$ are constants to be determined.

The form of (47) guarantees that the last two terms also satisfy the stationary stage equation $\frac{d^2 C_i}{d x^2} = 0$.

While the first term should be such that:

$$m_i(m_i - 1) a_i(x - x_i)^{m_i - 2} \tag{48}$$

be very small for x in the i -th phase. Form (47) is inspired by Goodman's method. So, the problem is to determine relationships between $m_i, a_i, b_i, c_i, i = 1, 2, 3$ such that conditions for decreasing and convexity of the concentration, for jump and null net flow in the interfaces are fulfilled. More exactly we write down:

$$C_1(x) = a_1(x - x_1)^m + b_1(x - x_1) + C_{\min}^1 \tag{49}$$

$$C_2(x) = a_2(x - x_2)^n + b_2(x - x_2) + C_{\min}^2 \tag{50}$$

$$C_3(x) = a_3(x - x_3)^m + b_3(x - x_3) \tag{51}$$

because C_{\min}^3 could be considered null. Forms (49-51)

guarantee:

$$C_1(x_1) = C_{\min}^1, C_2(x_2) = C_{\min}^2, C_3(x_3) = 0 \tag{52}$$

From the null net flow in the third interface it follows: $b_3 = 0$, so (49-51) take the form:

$$C_1(x) = a_1(x - x_1)^m + b_1(x - x_1) + C_{\min}^1 \tag{53}$$

$$C_2(x) = a_2(x - x_2)^n + b_2(x - x_2) + C_{\min}^2 \tag{54}$$

$$C_3(x) = a_3(x - x_3)^m \tag{55}$$

In straightforward fashion we got:

$$a_3 = (-1)^k \frac{C_{\max}^3}{(x_3 - x_2)^k} \tag{56}$$

$$b_2 = -k \frac{D_3}{D_2} \frac{C_{\max}^3}{(x_3 - x_2)} \tag{57}$$

$$a_2 = \frac{(-1)^n}{(x_2 - x_1)^n} [C_{\max}^2 - C_{\min}^2 - k \frac{(x_2 - x_1) D_3}{(x_3 - x_2) D_2} C_{\max}^3] \tag{58}$$

$$b_1 = \frac{D_2}{D_1} [\frac{(n-1)k}{(x_3 - x_2)} \frac{D_3}{D_2} C_{\max}^3 - \frac{n}{(x_2 - x_1)} (C_{\max}^2 - C_{\min}^2)] \tag{59}$$

$$a_1 = \frac{(-1)^m}{x_1^m} \{ C_s - C_{\min}^1 + x_1 \frac{D_2}{D_1} [\frac{(n-1)k}{(x_3 - x_2)} \frac{D_3}{D_2} C_{\max}^3 - \frac{n}{(x_2 - x_1)} (C_{\max}^2 - C_{\min}^2)] \} \tag{60}$$

A. Lemma.

Function $C(x) = a(x - x_0)^m + b(x - x_0) + c$, m integer greater or equal than two, is decreasing and convex in an interval $[x, x_0]$ if and only if:

$$\begin{cases} a \geq 0, b \leq 0 \text{ for } m \text{ even} \\ a \leq 0, b \leq 0 \text{ for } m \text{ odd} \end{cases} \tag{61}$$

Numerical experiments have been conducted to choose suitable values for m, n, k in (49-51).

VI. INVERSE PROBLEM OF COEFFICIENT IDENTIFICATION

To find diffusion coefficients $D_i, i=1,2$ we use the solution of (49-51) of the quasi-stationary problem and an optimization algorithm. We consider a generalized solution of the quasi-stationary problem in $H_0^1(0, x_3)$ and then minimize the functional associated to the norm in $H_0^1(0, x_3)$:

$$\begin{aligned}
 & J(a_1, a_2, a_3, b_1, b_2) \\
 &= \int_0^{x_1} |m(a_1(x-x_1)^{m-1} + b_1 + \frac{C_s - C_{\min}^1}{x_1})|^2 dx + \\
 & \frac{D_2}{D_1} \int_{x_1}^{x_2} |n(a_2(x-x_2)^{n-1} + b_2 + \frac{C_{\max}^2 - C_{\min}^2}{x_2 - x_1})|^2 dx + \\
 & \frac{D_3}{D_1} \int_{x_2}^{x_3} |k(a_3(x-x_3)^{k-1} + b_3 + \frac{C_{\max}^3}{x_3 - x_2})|^2 dx \quad (62)
 \end{aligned}$$

subject to the restrictions:

$$\begin{aligned}
 & b_i \leq 0, \quad i=1,2,3 \\
 & |a_i| \leq \varepsilon, \quad i=1,2,3 \quad (63)
 \end{aligned}$$

(ε small enough for the associated profile to be quasi-stationary)

$$\begin{aligned}
 & a_1(-x_1)^m - bx_1 + C_{\min}^1 = C_s \\
 & a_2(x_1 - x_2)^n + b_2(x_1 - x_2) + C_{\min}^2 = C_{\max}^2 \quad (64) \\
 & a_3(x_2 - x_3)^k = C_{\max}^3
 \end{aligned}$$

$$a_1 \begin{cases} \leq 0, m \text{ odd} \\ \geq 0, m \text{ even} \end{cases} \quad (65)$$

$$a_2 \begin{cases} \leq 0, n \text{ odd} \\ \geq 0, n \text{ even} \end{cases} \quad (66)$$

$$a_3 \begin{cases} \leq 0, k \text{ odd} \\ \geq 0, k \text{ even} \end{cases} \quad (67)$$

which allows to find approximate values of $\frac{D_2}{D_1}, \frac{D_3}{D_2}$

VII. NUMERICAL EXPERIMENTS

They were done in a PC at 900 Mhz, using Matlab version 6.5 regression programs. Results were compared to those obtained in a traditional fashion.

Experiments yield that:

- a) Estimate is not sensitive to the increase of the number of measurements in the third phase.
- b) Estimate is very sensitive to the initial vector. It seems that an initial value of D_3/D_1 near to 1000 is the best option,

while for D_2/D_1 it does not matter the initial value when no errors are considered.

c) Estimate needs at least two large weight coefficients in the objective function. One in the first or second phase and the other in third one when no errors are considered.

d) Estimate is sensitive to measurement errors. A regularization process is needed to improve results.

e) More numerical experiments are needed to confirm these preliminaries conclusions.

ITER	IFUN	FMIN	G
0	1	130.46699365	148844719.91815180
1000	1002	3.95163563	4589.43828985
2000	2002	1.34832675	265.05001931
3000	3004	0.02426624	26808.27486805
4000	4004	0.00077306	653.60070554
4320	4324	0.00000000	0.00000190

TERMCODE = 0 - Convergence to a local minima.
 Fdif 1 = 0.000007 Udif 1 = 0.000007.

ACKNOWLEDGMENT

J. Bernal, S. Rangel and A. Juanico thanks the support provided by PROMEP and UPVM to carry out this work.

REFERENCES

- [1] J. Grosch, J. Morral, M. Scheider, Proc. Second Conf. Carburizing and Nitriding with Atmospheres, ASM International, 1995.
- [2] T. Bell and H. Thomas, Cyclic Stressing of Gas Nitrocarburized low carbon Steel, *Metallurgical Transactions A*, Vol. 10, No. 1, 1979, pp. 79-84.
- [3] B. M. Karamis and E. Gerçekcio, Wear behavior of plasma nitrided steels at ambient and elevated temperatures, *Wear*, Vol. 243, 1-2, 2000, pp. 76-84.
- [4] Zbigniew Łataś, Aleksander Ciski & Pavel Šuchmann Comtes, Cryogenic Treatment and Combination of Nitriding and Cryogenic Treatment of Hot Forging Tools, *Proceedings of the 4th WSEAS Int. Conf. on Heat Transfer, Thermal Engineering and Environment*, Elounda, Greece, August 21-23, 2006, pp. 133-139.
- [5] J. Bernal-Ponce, A. Fraguera-Collar, J. A. Gómez, J. Oseguera-Peña, F. Castillo Aranguren, Identification of diffusion coefficients during post-discharge nitriding, *Proceedings of the 5th International conference on Inverse Problems in Engineering: Theory and Practice*, Cambridge, UK, Vol. 1, 2005, B05.
- [6] J. Crank, *The Mathematics of Diffusion*, 2nd ed. Oxford Science Publications, 1993.
- [7] J. Crank, *Free and Moving Boundary Problems*, Clarendon Press Oxford. 1984.
- [8] E. Javierre-Pérez, *Numerical methods for solving Stefan problems*, Report 03-16, Department of Applied Mathematical Analysis, delft University of Technology, 2003.
- [9] A. Marciniak, Equilibrium and non equilibrium models of layer formation during plasma and gas Nitriding, *Surface Engineering*, Vol. 1, 1985, pp. 283-287.
- [10] M.A.J. Somers and Mittemeijer, Layer-Growth Kinetics on Gaseous Nitriding of Pure Iron: Evaluation of Diffusion coefficients for Nitrogen in Iron Nitrides, *Metallurgical and Materials Transactions*, Vol. 26, No. 1, 1995, pp. 57-74.
- [11] H. Du and J. Agren, Z. Gaseous Nitriding Iron –Evaluation of Diffusion Data of N in γ' and ϵ Phases, *Metallkd.*, Vol. 86, No. 8, 1995, pp. 522–529.
- [12] H. Wilhelmi, S. Strämke, Pohl, H.C.: Nitrieren mit gepulster Glimmentladung Härtereitechn. *Mitteilungen* 37, 6, 1982, S. 263 - 310.
- [13] Strämke, S.; Stein, W.: Pulsation Improves Results in Plasma Nitriding *Wire World International*, Vol. 26, March/ April 1984.

- [14] M. Samandi, B.A. Shedden, D.I. Smith, G.A. Collins, R. Hutchins, S. Tendys, *Surf. Coat. Technol.* 59, 1993, 261.
- [15] E. Rolinski, Effect of plasma nitriding temperature on surface properties of stainless steel *Surf. Eng.* 3, 1, 1987, 35-40.
- [16] Z. L. Zhang, T. Bell, Structure and corrosion resistance of plasma nitrided stainless steel *Surf. Eng.* 1, 2, 1985, 131.
- [17] O. Knotek, et al., *Proc. 1st Intern. Conf. Surf. Eng.*, Brighton, England, 25-28 June, 1985.
- [18] A. Wells, I. Le, R. Strydom, Sputtering and Redeposition of Cathode Material during Plasma Nitriding, *Surf. Eng.*, 2, 4, 1986, pp. 263-267.
- [19] Torchane, P. Bilinger, J. Dulcy and M. Gantois, Control of Iron Nitride Layers Growth Kinetics in the Binary Fe-N System, *Metallurgical and Materials Transactions*, Vol. 27A, No. 7, 1996, pp. 1823-1835.
- [20] M. Yan, J. Yan and T. Bell, Numerical Simulation of Nitride Layer growth and nitrogen distribution in ϵ , γ' and α Fe during pulse plasma nitriding of pure iron, *Modeling Simul. Mater. Sci. Eng.*, Vol. 8, 1996, pp. 491-496.
- [21] U. Figueroa, J. Oseguera, P.S. Shabab-Retchkiman, Growth kinetics of concomitant nitride layers in postdischarge conditions: modeling and experiment, *Surf. Coat. Technol.*, Vols. 86-87, 1996, pp. 728-734.
- [22] S. K. Lee and H.C. Shih, Structure and Corrosive Wear Resistance of Plasma-Nitrided Alloy Steels in 3% Sodium Chloride Solutions, *Corrosion*, Vol. 50, No. 11, 1994, pp. 848-856.
- [23] K. Scwerdtfeger, P. Grieveson and E.T. Turkdogan, Growth Rate of Fe₄N on Alpha iron in NH₃-H₂ Gas Mixtures: Self-Diffusivity of Nitrogen, *Transactions of the Metallurgical Society of AIME*, Vol. 245, 1969, pp. 2461-2466.
- [24] J.L. Bernal, O. Salas, U. Figueroa, and J. Oseguera, Early stages of γ' nucleation and growth in a post-discharge nitriding reactor, *Surf. Coat. Technol.*, Vols. 177-178, 2004, pp. 665-670.
- [25] S. T. Belmonte, S. Bockel, H. Michel D. Ablitzer, Study of transport phenomena by 3D modeling of a microwave post-discharge nitriding reactor, *Surf. Coat. Technol.*, Vol. 112, 1999, pp. 5-9.
- [26] A. Ricard, M. Gaillard, V. Monna, A. Vesel and M. Mozetic, Excited species in H₂, N₂, O₂, microwave flowing discharges and post-discharges, *Surf. Coat. Technol.*, Vols. 142-144, 2001, pp. 333-336.
- [27] A. Ricard, J.E. Oseguera Peña, L. Falk, H. Michel and M. Gantois, Active Species in Microwave post-discharge for steel surface nitriding, *IEEE Trans. Plasma Sci.*, Vol. 18, No. 6, 1990, pp. 940-943.

J. Bernal was Born in Atlixco Puebla., México, in 1968. He studied Materials Science and Engineering at the Instituto Tecnológico y de Estudios Superiores de Monterrey in México, and he took his degree in 2000. In 2006 he graduated his doctoral degree from the Instituto Tecnológico y de Estudios Superiores de Monterrey in México. His doctoral thesis was focused on the characterization and Modeling of nitrided materials on postdischarge conditions. He is working now as research professor at the Universidad Politécnica del Valle de México. His research activities are focused on materials Characterization and Modeling.